Check for updates

DOI: 10.1049/ccs2.12041

ORIGINAL RESEARCH



Fast Fourier transform and wavelet-based statistical computation during fault in snubber circuit connected with robotic brushless direct current motor

Sankha Subhra Ghosh¹



| Arabinda Das³

Correspondence

Surajit Chattopadhyay, Department of Electrical Engineering, GKCIET, Malda, West Bengal 732141,

Email: surajitchattopadhyay@gmail.com

Abstract

The snubber circuit plays an important role in motor drives. This paper deals with the detection of the inverter switch snubber circuit resistance fault (ISSCRF) in brushless direct current (BLDC) motors used for robotic applications. This has been carried out in two parts: Fast-Fourier-Transform-based analysis and wavelet-decomposition-based analysis on the stator current of the BLDC motor. The first analysis investigates the effects of different percentages of ISSCRF on direct current (DC) component, fundamental frequency component and total harmonic distortion percentage. Next analyses consider all of kurtosis, skewness and root-mean-square values of wavelet coefficients of stator current harmonic spectra. Comparative learning is made to obtain a few selective parameters best fit for the detection of ISSCRF. A fault detection algorithm to detect ISSCRF has been proposed and validated by three case studies. The algorithm is again modified with best-fit parameters. Comparative discussion and novel contributions of the work have also been presented.

KEYWORDS

Brushless DC motor, discrete wavelet transform (DWT), fault diagnosis, inverter switch snubber circuit

INTRODUCTION

Brushless direct current (BLDC) motors are electronically commutated motors that provide high efficiency, good dynamic response, high mechanical reliability, low noise and vibration, long lifetime, and easy controllability [1]. These motors are widely used nowadays in servo drives, transport systems, medical instruments, industrial, residential applications [1, 2]. Also, their use can be found in aerospace, military and robotic applications. In the BLDC motor, there is no presence of brushes, whereas brushes can be found attached with the stator in a conventional DC motor [3]. A three full-bridge inverter is used to drive a three-phase BLDC motor [4]. In spacecraft applications, the sensorless BLDC motor is used, as the system reliability can be decreased due to the use of hall devices as discrete position sensors [4, 5]. Also in recent days, position, sensorless BLDC motors are mostly used. Several types of faults may happen at stator, rotor, position sensors or voltage

source inverter (VSI) in a BLDC motor drive [6]. So, if these faults are not detected, they may cause severe machine failures. For fault diagnosis, several techniques have been used recently like fast Fourier transform (FFT), short-time Fourier transform (STFT), and wavelet transform.

Three basic classifications for fault detection and diagnosis algorithms of a BLDC motor are signal analysis, model-based, and knowledge-based methods [6, 7]. In the first method, there is no need for a dynamic model of the motor, in this method, the features of the output signal are extracted, which are further used for the detection of the faults; but, this fault detection is not fast as other methods [6]. To detect and diagnose faults, parameter estimation techniques are used in the second method that can be used for online fault detection but it requires the exact model of the motor [6]. In the third method, based on experienced knowledge, expert systems are developed using a fuzzy logic or a neural network to detect and diagnose motor faults [7]. For continuous and safe operation,

This is an open access article under the terms of the Creative Commons Attribution-NonCommercial-NoDeriys License, which permits use and distribution in any medium, provided the original work is properly cited, the use is non-commercial and no modifications or adaptations are made.

© 2022 The Authors. Cognitive Computation and Systems published by John Wiley & Sons Ltd on behalf of The Institution of Engineering and Technology and Shenzhen University.

¹Department of Electrical Engineering, IMPS College of Engineering and Technology, Malda, West

²Department of Electrical Engineering, GKCIET, Malda, West Bengal, India

³Department of Electrical Engineering, Jadavpur University, Kolkata, India

motors should remain stable and operate as per the control logic applied to the actuator to achieve the reliable performance of a control system [8]. Power inverter failures are about 38% of the total motor failures and these faults mainly occur in power switches [9].

Various techniques have been researched and proposed for the detection of inverter switch faults in BLDC motors during recent decades. In 2016, Mehdi Salehifar et al. have proposed a fault detection technique for an open-switch and short-circuit faults in VSI [10]. Mehdi Salehifar et al. also proposed a technique to detect faulty switches in a fivephase VSI supplying motor drive [11] in 2016. In 2011, Byoung-Gun Park et al. adopted a simple algorithm for phase current measurement and introduced an open-switch fault diagnosis scheme for the BLDC motor drives [12]. But, the fault diagnosis method proposed in [12] can trigger a false alarm especially in the motor with a small operating current because of the measurement noise [13]. Mohamed A. Awadallah et al. in 2006 proposed a diagnostic technique for a current-source inverter fed Permanent Magnet (PM) BLDC motor drives to detect open-switch faults on the inverter bridge using wavelets and neuro-fuzzy systems through a discrete-time lumped-parameter network model [14]. A model-based fault detection technique applicable for end-of-line and online fault detection [15] was proposed by Moseler et al. in 2000. But as per Wang et al. [16], the results obtained from these fault detection techniques are influenced by model uncertainties, system faults. Due to the unpredictable and unknown uncertainties, these cannot be mathematically modelled, which further resulted in the differences between the results obtained from the simulation and performance of the actual system and provides wrong results in the fault detection technique based on the model [17]. In 2000, Liu et al. showed the parameter estimation and the neural network fault diagnosis system [7].

The wavelet-decomposition-based motor current signature analysis was made for motor fault diagnosis using statistical parameters [18] such as kurtosis, skewness, root-mean-square (RMS) etc. But, an attempt by utilising these parameters for the detection of inverter switch snubber circuit resistance fault (ISSCRF) of the BLDC motor is very few. In power, an electronic circuit snubber plays an important role. Snubbers are found in the power supply unit. It is a small circuit in the power switching module, which is very efficient in controlling the effects of the circuit reactance. By doing so, snubber not only improves the switching circuit's performance but also increases the reliability and efficiency and also results in a higher switching frequency [19]. It also results in lower electromagnetic interference (EMI) in other circuits. In switching devices, a sharp rise in the voltage may appear that may result in sudden interruption and can damage the switching devices.

The performance of the BLDC drive has been analysed with and without a snubber [20, 21]. For reliable operation of drives, fault diagnosis is an important aspect that should be paid attention to. A lot of study and research is going on in this field [21–25] for fault diagnosis of the converter and motor drives. Useful mathematical tools were presented in

[22]. Most of the fault diagnosis methods deal with motor faults [22, 24, 25]. Starting transients have been found very effective for motors' fault diagnosis [23]. Many advanced modelling, study and applications of the snubber have been observed [26–32]. Faults in the converter connected with the snubber were detected [26] and the new protective scheme was modelled [27]. Performance of converter was been analysed in [28–32]. However, it is important to note that no literature has been observed that directly deals with the detection of fault that occurs in the snubber itself. This has motivated us to deal with the diagnosis of the fault that occurred in the snubber circuit.

1.1 | Snubber resistance fault

In this work, a resistance-capacitance (RC) snubber circuit has been considered for the fault analysis. RC snubbers used with inductive loads such as electric motors commonly use a small resistor in series with a small capacitor. This limits the rate of rising in voltage (dV/dt) across the thyristor to a value that prevents the inaccurate turn-on of the thyristor. 'Snubber resistance fault' may occur due to ageing, temperature and other factors. The snubber itself plays a key role in the minimisation of electromagnetic levels and mitigation of voltage spikes on the switches. Snubber resistance fault refers to damage to the snubber resistor. It initiates from the gradual decrease of the effective resistance value of the snubber resistor. Under the extreme condition, it becomes zero and the snubber path gets short-circuited. This short-circuit condition of the snubber path is easy to detect. But, the gradual decrease of the snubber resistance is difficult to detect. Ignorance of this may cause larger damage and greater repairing time. Therefore, in this work, an attempt has been taken to detect a small and gradual decrease in the resistance value of the snubber resistor. The value of the snubber resistor beyond the 5% tolerance range has been considered here as the fault level. It may be noted that the selection of the fault level depends on designers' choices and the system specifications.

If the ISSCRF occurs, it should be detected to prevent the system from further expensive damage.

1.2 Workflow

In this work, the stator current drawn by the BLDC motor is analysed during ISSCRF. Monitoring of the parameters such as DC component, fundamental component, total harmonic distortion (THD) of the stator current based on the FFT and wavelet-decomposition-based kurtosis, skewness and RMS values of approximate and detail coefficients has been done for fault diagnosis. Also, an algorithm has been proposed, which has been validated at the end.

The paper has been organised into seven sections. After the introduction, mathematical modelling of BLDC motor, inverter switch and snubber circuit has been presented in Section 2. Section 3 deals with the FFT-based analysis. Then,

to overcome the limitations of the FFT-based analysis, a wavelet-based statistical analysis has been carried out in Section 4. Then, an algorithm has been proposed, case studies have been made and validations have been done in Section 5. Comparisons and novel contributions of the work have been presented in Section 6 followed by the conclusion in Section 7. Authors have studied a 5%–50% decrease in the snubber resistance. Both simulation and experimental case studies have been carried out. In the simulation, 1% incremental value from 5% to 50% decrease of the effective resistance value has been considered. In experimental case studies, three different fault values were available that have been considered for validation.

2 | BLDC MOTOR MATHEMATICAL MODELLING AND INVERTER SWITCH SNUBBER CIRCUIT DESIGN

2.1 | Mathematical model of the BLDC motor

The equivalent circuit of the BLDC motor has been shown in Figure 1. The BLDC motor has three stator windings in star connection, which is fed by a three-phase voltage source.

If V_a , V_b , and V_c are the stator phase voltages in volts, i_a , i_b , and i_c are the stator phase currents in amperes and e_a , e_b , and e_c are the motor back EMFs in volts for phases a, b and c, respectively, then BLDC motor armature winding modelling may be expressed as follows:

$$V_a = Ri_a + L\frac{di_a}{dt} + e_a \tag{1}$$

$$V_b = Ri_b + L\frac{di_b}{dt} + e_b \tag{2}$$

$$V_c = Ri_c + L\frac{di_c}{dt} + e_c \tag{3}$$

The modelling of the BLDC motor may be expressed in a matrix form as follows:

$$\begin{bmatrix} V_{a} \\ V_{b} \\ V_{c} \end{bmatrix} = R \begin{bmatrix} 1 & 0 & 0 \\ 0 & 1 & 0 \\ 0 & 0 & 1 \end{bmatrix} \begin{bmatrix} i_{a} \\ i_{b} \\ i_{c} \end{bmatrix} + L \begin{bmatrix} 1 & 0 & 0 \\ 0 & 1 & 0 \\ 0 & 0 & 1 \end{bmatrix} \frac{d}{dt} \begin{bmatrix} i_{a} \\ i_{b} \\ i_{c} \end{bmatrix} + \begin{bmatrix} e_{a} \\ e_{b} \\ e_{c} \end{bmatrix}$$
(4)

where $R = R_a = R_b = R_c$ is the per phase stator resistance in ohm. $L = L_a = L_b = L_c$ is the per phase inductance of the stator winding

For modelling eight poles, 3000 revolutions per minute (RPM) BLDC motor has been considered in this work. The motor's stator phase resistance and stator phase inductances are $2.8750~\Omega$ and 0.0085~H, respectively. The rotor inertia and

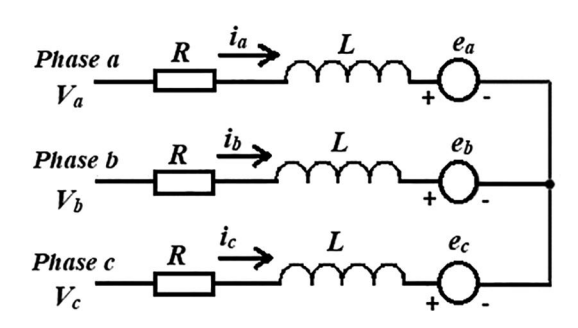


FIGURE 1 Equivalent circuit of a brushless direct current motor

friction values are 0.008 kg m² and 0.001 N m s, respectively. A 3-phase, 500 V, 50 Hz supply unit that includes a MOSFET/Diodes-based inverter has been used to energise the motor. Monitoring on the stator current has been done for the normal condition and different percentages of ISSCRF (up to 50%).

2.2 | Inverter switch snubber circuit design

To achieve better performance and protection, snubber circuits are used across the semiconductor switches. Turn on time of semiconductor switches is 10-100 µs, which causes the fall of voltage across these switches and the current through these switches also rises during this time. A rapid change in voltage and current may often damage the semiconductor switches [20]. Generally, snubbers are used in load line shaping so that they can remain within the safe operating area. It reduces losses during the switching time, limits dv/dt and di/dt, ripples. Voltage and current spikes are also reduced using the snubber circuit. Snubbers are also used for reducing the heat in the device [20]. A series-connected resistor with a capacitor connected in shunt with the semiconductor switch is the basic circuit of a snubber circuit. Snubbers slow down the rate of rising of the current through the semiconductor switch [20]. It is used for the reduction of the peak voltage value at turn-off and it also damps the oscillation of the signal. The change in current can be opposed by connecting an inductor in series with the semiconductor switch [20]. In this work, the RC snubber circuit used in the inverter circuit of the BLDC motor has been shown in Figure 2.

Calculation of the snubber resistance and snubber capacitance values can be done using the following formulae [21]:

$$R_{\rm snub} = 2.\delta \sqrt{\frac{L}{C}} \tag{5}$$

$$C_{\text{snub}} = L \left(\frac{I_r}{K \cdot V_S} \right)^2 \tag{6}$$

where $R_{\rm snub}$ = snubber resistance, $C_{\rm snub}$ = snubber capacitance, δ = optimum damping factor, K = optimum current factor, I_r = recovery current of the semiconductor switch, V_s = source voltage, and L = circuit inductance.

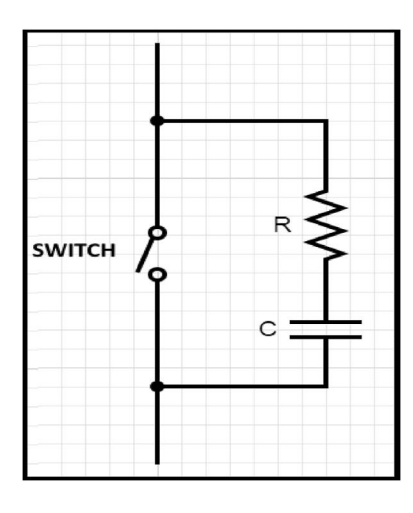


FIGURE 2 Inverter switch RC snubber circuit of the brushless direct current motor

3 | FFT-BASED FAULT DIAGNOSIS

For the analysis of a periodic waveform, Fourier transform (FT) is an efficient tool. A signal is converted into the frequency domain from the time domain by both FT and FFT. However, FFT is very fast as it requires a very less number of computations as compared to the FT. It provides information related to the different frequency components that are present in the signal. FFT is applied to the current signal of a motor if it is in a steady-state running condition. According to the researchers, the FFT analysis can identify the exact extent of defects as well as the associated frequencies [22]. The sampling rate used in the FFT-based analysis was 100 kS/s.

3.1 | Analysis of the DC component

The FFT-based analysis has been done on the stator current of the BLDC motor to extract the DC component for different percentage values of ISSCRF as shown in Figure 3. It shows that the DC component of the stator current varies as the percentage of ISSCRF varies. But from Figure 3, no exact relation between the DC component of the stator current and different percentages of ISSCRF has been observed.

3.2 | Analysis of the fundamental component

To analyse the frequency pattern of the stator current in the BLDC motors, a fundamental frequency calculation is required. The fundamental component of the stator current has been extracted and studied for different percentage values of ISSCRF as shown in Figure 4.

From Figure 4, it can be observed that ISSCRF distorts the stator input current. Here also, no exact relation between the fundamental frequency component of stator current and different percentage values of ISSCRF has been observed.

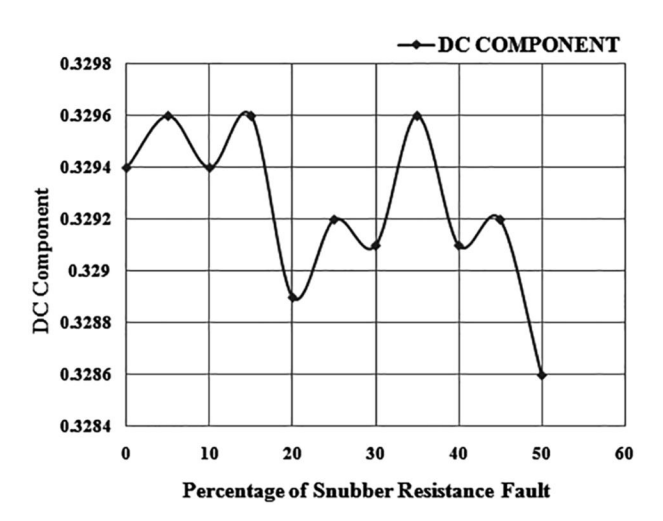
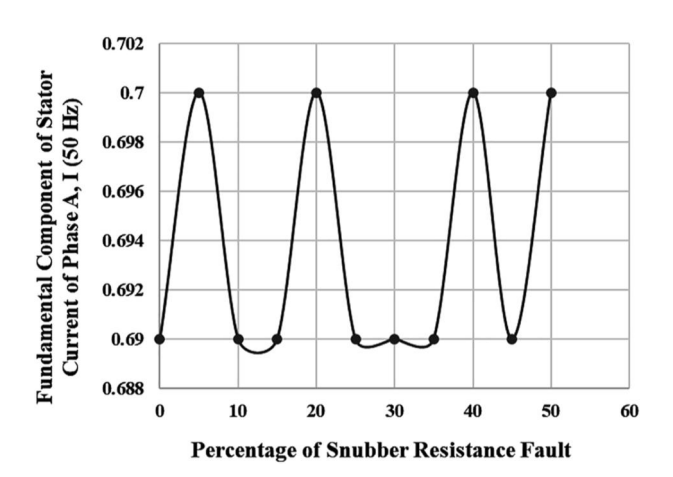


FIGURE 3 DC component versus percentage of inverter switch snubber circuit resistance fault



25177676, 2022. I, Downoaded from thtps://ietresearch.onlinelibrary.wiely.com/doi/10.1049/ccs2.12041, Wiley Online Library on [2404/2024]. See the Terms and Conditions (https://onlinelibrary.wiely.com/retrms-and-conditions) on Wiley Online Library for rules of use; OA articles are governed by the applicable Creative Commons Licensean Conditions (https://onlinelibrary.wiely.com/retrms-and-conditions) on Wiley Online Library for rules of use; OA articles are governed by the applicable Creative Commons Licensean Conditions (https://onlinelibrary.wiely.com/retrms-and-conditions) on Wiley Online Library for rules of use; OA articles are governed by the applicable Creative Commons Licensean Conditions (https://onlinelibrary.wiely.com/retrms-and-conditions) on Wiley Online Library for rules of use; OA articles are governed by the applicable Creative Commons Licensean Conditions (https://onlinelibrary.wiely.com/retrms-and-conditions) on Wiley Online Library for rules of use; OA articles are governed by the applicable Creative Commons Licensean Conditions (https://onlinelibrary.wiely.com/retrms-and-conditions) on Wiley Online Library for rules of use; OA articles are governed by the applicable Creative Commons Licensean Conditions (https://onlinelibrary.wiely.com/retrms-and-conditions) on Wiley Online Library for rules of use of use

FIGURE 4 Fundamental component of the stator current versus the percentage of inverter switch snubber circuit resistance fault

3.3 | Analysis of total harmonic distortion (THD)

The ratio of the RMS of all the harmonic contents to the rootmean-square value of the fundamental quantity is known as THD; it is expressed by the percentage of the fundamental. To find out the amount of distortion of a voltage or current due to harmonics in the signal can be measured by finding out the THD of that signal. THD may be expressed as

$$THD = \frac{\sqrt{\sum_{n=2}^{\infty} I_{n_rms}^2}}{I_{fund_rms}}$$
 (7)

where I_{n_rms} and I_{fund_rms} are the RMS values of the *n*th harmonic and the fundamental frequency, respectively. For the ISSCRF fault analysis, THD values of the stator current have been extracted as shown in Figure 5. It can be observed from Figure 5 that the THD values vary with the variation in the percentage of ISSCRF. However, from Figure 5, no exact

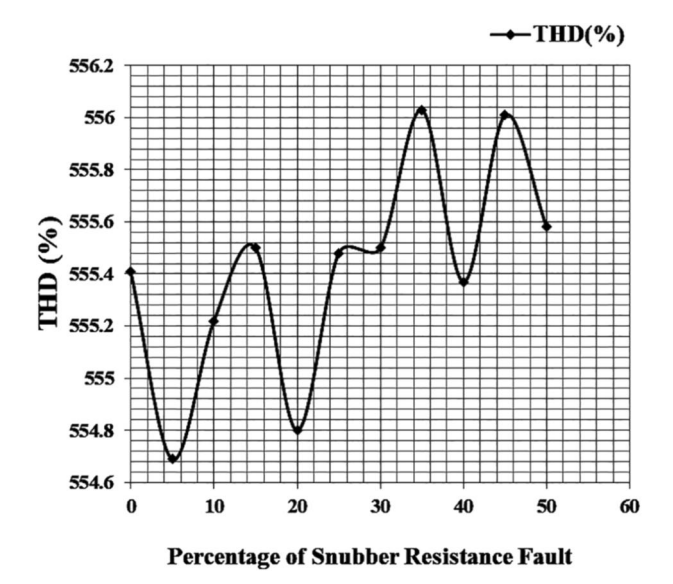


FIGURE 5 Total harmonic distortion (%) versus percentage of inverter switch snubber circuit resistance fault

relation between the changes in THD (%) with the changes in the percentage of ISSCRF has been observed.

3.4 | Limitation

It has been observed that FFT-based fault diagnosis done here for the detection of ISSCRF of a BLDC motor has not provided any meaningful conclusion, which can be used for the assessment of ISSCRF. So, FFT is inappropriate where the signal's characteristic changes with time because the time information is lost during the transformation of a signal from the time domain to the frequency domain, which is a major limitation of this method [22]. Here, it has been observed as the stator current is transient in nature, FFT-based fault diagnosis becomes an inappropriate method to detect ISSCRF of a BLDC motor. Also according to the authors in [22, 23], the FFT does not give the correct result when the motor current is non-stationary in nature. To overcome the limitation of FFT, in Section 4, wavelet-transform-based fault diagnosis has been done.

4 | DISCRETE WAVELET TRANSFORM (DWT)-BASED FAULT DIAGNOSIS

To deal with non-stationary signals, the wavelet transform is a very effective tool [18]. As the signals are captured in a discrete form, DWT will be suitable for the analysis [22]. The integer number of discrete steps in scale and translation denoted by m and n, respectively, decides the number of wavelet coefficients provided by DWT and if segmentation step sizes for the scale and translation are a_0 and b_0 , respectively, then for these parameters, the scale and translation of RMS will be $a = a_0^m$ and $b = nb_0a_0^m$. Hence, the discrete wavelet coefficients are given by

$$DWT(m,n) = \int_{-\infty}^{\infty} \frac{1}{\sqrt{a_0^m}} f(t) g(a_0^{-m} t - nb_0) d(t)$$
 (8)

where $g(a_0^{-m}t - nb_0)$ is the discrete wavelet with scale and translation.

In this work, the stator current of phase-A of the BLDC motor has been extracted for the analysis. DWT has been applied to decompose the extracted current up to the DWT level 9. Here, Daubechies wavelet 'db4' has been considered as a mother wavelet. Approximate and detail coefficients up to the ninth decomposition level have been determined for normal and faulty conditions (up to 50%) of ISSCRF. In Figure 6, few results have been shown from the total results obtained, where the first row of the first column and the second row of the second column show the extracted signal corresponding to the stator current of phase A and the succeeding rows after the first row of the first column and the succeeding rows after the second row of the second column show the approximate and detail coefficients for decomposition level up to ninth.

From the graphical assessment technique presented in Figure 6, it is not easy to distinguish between different percentages of ISSCRF as all the graphical results appeared to be the same here. So, from this analysis, no exact conclusion can be drawn, which can be used further to detect the ISSCRF. To do the assessment better and for the detection of ISSCRF of a BLDC motor kurtosis, skewness and RMS values of the harmonic spectrum of the stator current up to the ninth DWT level have been determined.

4.1 | Statistical parameters under consideration

In this section, wavelet decomposition coefficients are denoted as follows: (a) the kurtosis values of approximate and detailed coefficients are denoted by A_K , D_K , (b) the skewness values of approximate and detailed coefficients are denoted by A_S , D_S and (c) the RMS values of approximate and detailed coefficients are denoted by A_R , D_R . The kurtosis values of approximate and detailed coefficients up to the ninth DWT level may be expressed as

$$[k] = \begin{bmatrix} [A_K] \\ [D_K] \end{bmatrix}$$

$$= \begin{bmatrix} A_{K1} & A_{K2} & A_{K3} & A_{K4} & A_{K5} & A_{K6} & A_{K7} & A_{K8} & A_{K9} \\ D_{K1} & D_{K2} & D_{K3} & D_{K4} & D_{K5} & D_{K6} & D_{K7} & D_{K8} & D_{K9} \end{bmatrix}$$

$$(9)$$

The skewness values of approximate and detailed coefficients up to the ninth DWT level may be expressed as

$$[s] = \begin{bmatrix} [A_S] \\ [D_S] \end{bmatrix}$$

$$= \begin{bmatrix} A_{S1} & A_{S2} & A_{S3} & A_{S4} & A_{S5} & A_{S6} & A_{S7} & A_{S8} & A_{S9} \\ D_{S1} & D_{S2} & D_{S3} & D_{S4} & D_{S5} & D_{S6} & D_{S7} & D_{S8} & D_{S9} \end{bmatrix}$$

$$(10)$$

25177567, 2022. 1, Downloaded from https://ietresearch.onlinelibrary.wiley.com/doi/10.1049/ccs2.12041, Wiley Online Library on [2404/2024]. See the Terms and Conditions (https://onlinelibrary.wiley.com/errns-and-conditions) on Wiley Online Library for rules of use; OA articles are governed by the applicable Creative Commons. Licensed

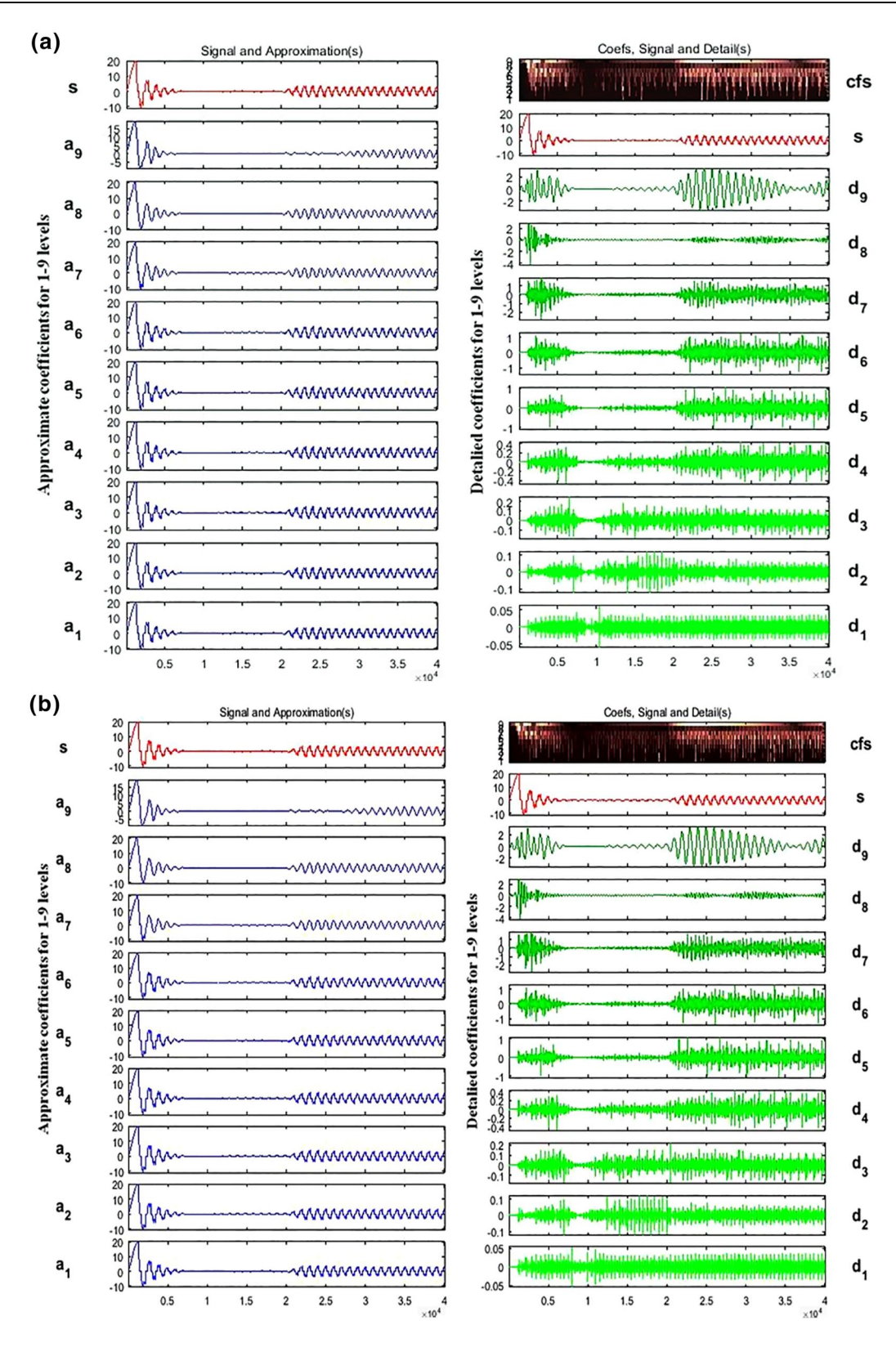


FIGURE 6 Approximate and detailed coefficients at different percentages of inverter switch snubber circuit resistance fault. (a) under normal condition, (b) at 5% fault

37

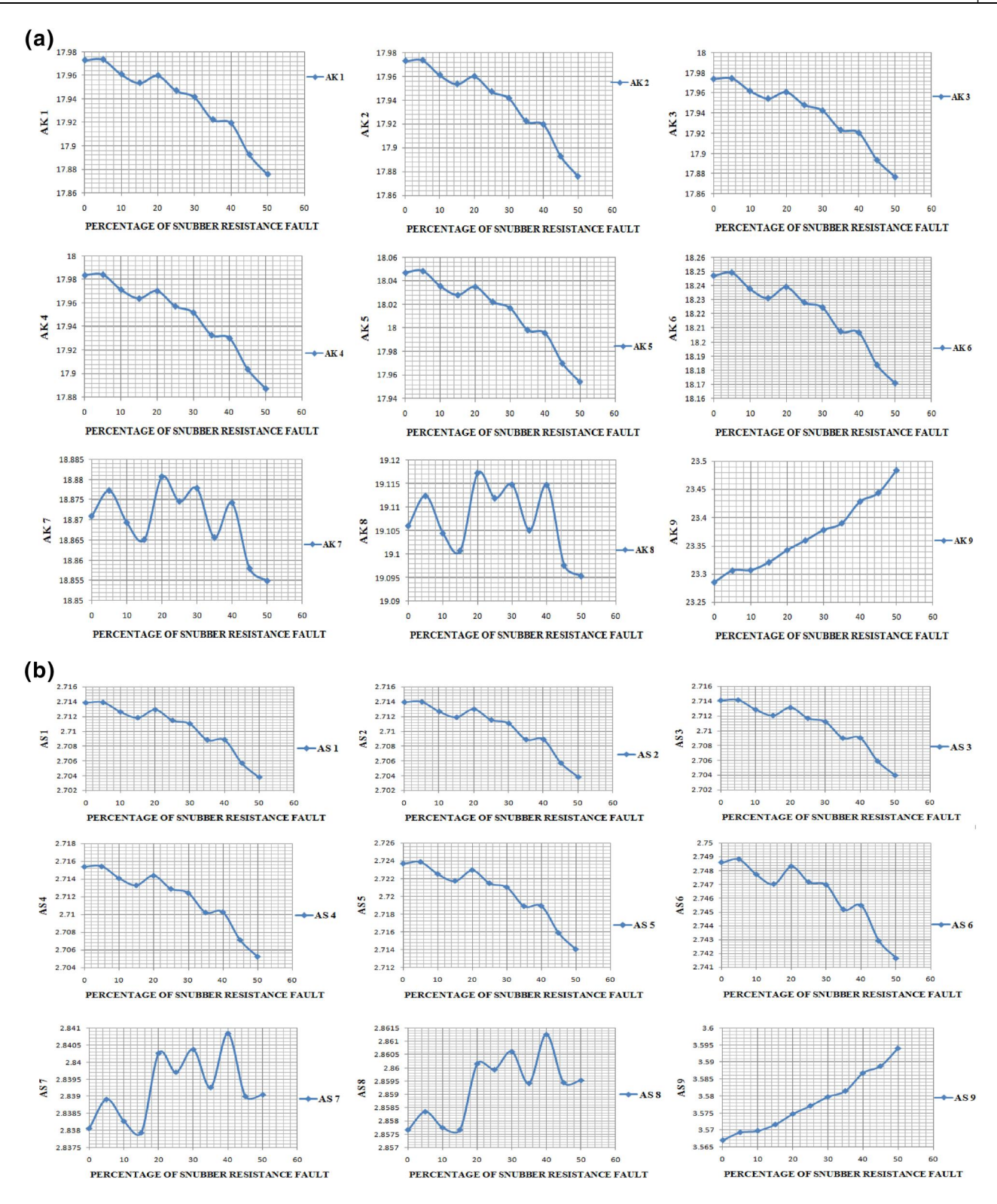


FIGURE 7 Kurtosis, skewness, RMS values of approximate coefficients versus percentage of inverter switch snubber circuit resistance fault (ISSCRF).

(a) Kurtosis values of approximate coefficients versus the percentage of ISSCRF. (b) Skewness values of approximate coefficients versus the percentage of ISSCRF.

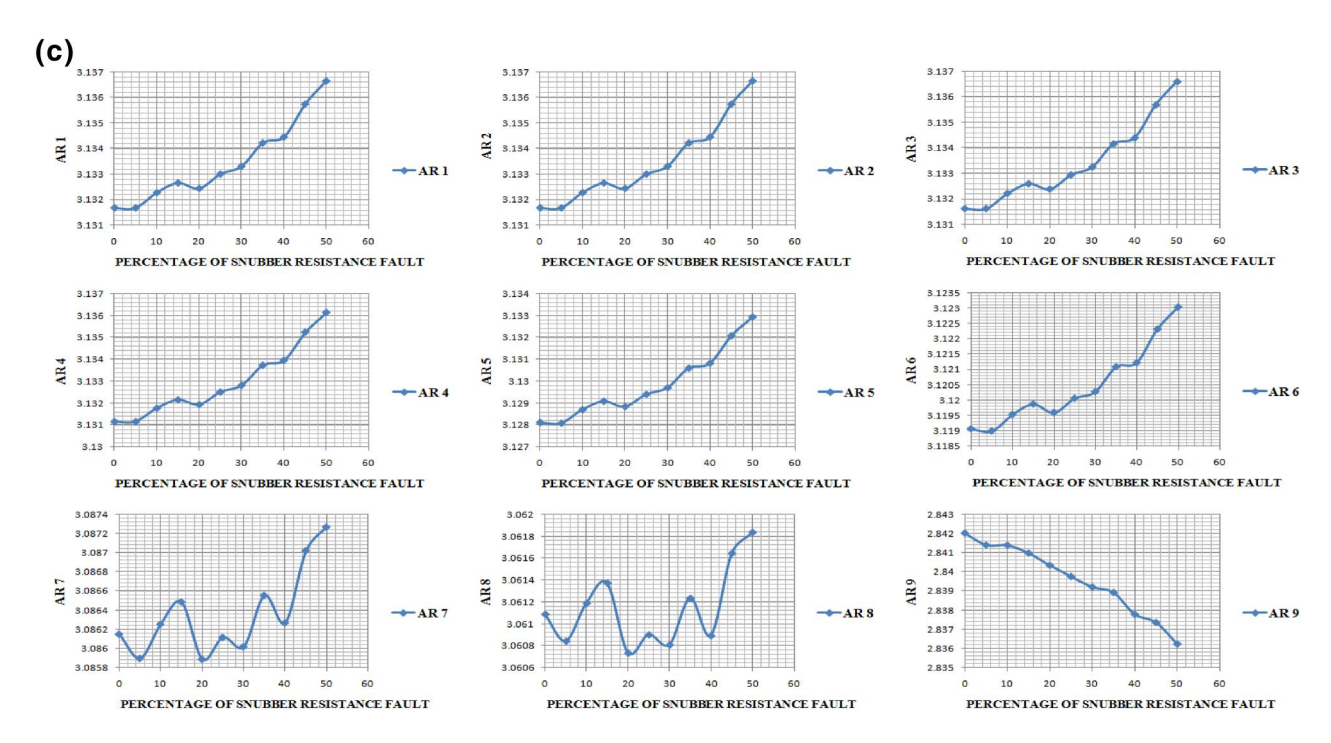


FIGURE 7 (Continued)

The RMS values of approximate and detailed coefficients up to the ninth DWT level may be expressed as

$$[R] = \begin{bmatrix} [A_R] \\ [D_R] \end{bmatrix}$$

$$= \begin{bmatrix} A_{R1} & A_{R2} & A_{R3} & A_{R4} & A_{R5} & A_{R6} & A_{R7} & A_{R8} & A_{R9} \\ D_{R1} & D_{R2} & D_{R3} & D_{R4} & D_{R5} & D_{R6} & D_{R7} & D_{R8} & D_{R9} \end{bmatrix}$$

$$(11)$$

Statistical parameters have been found effective in current signature analysis and diagnosis of BLDC motor faults that produce non-stationary signals.

4.2 | Assessment of statistical parameters for approximate coefficients

For the normal condition and for different percentages of ISSCRF conditions of the BLDC motor, A_K , A_S , and A_R have been determined, which have been shown in Figure 7.

As shown in Figure 7, it can be observed that A_K values for the first level to the sixth level have close similarities and from the nature obtained from these values, any effective conclusion cannot be drawn. The A_K values for the seventh and eighth levels are very zig-zag in nature and it is not providing any effective conclusion for fault diagnosis. The same properties can be seen in case of the values for A_S , A_R which also are not effective for fault diagnosis. But from Figure 7, it can be observed that both the values of A_K , A_S at decomposition level 9 are increasing and only the value of A_R at the 9th decomposition level is decreasing with the

increase in the percentage of ISSCRF. Thus, A_K , A_S and A_R at decomposition level 9 can be helpful for fault assessment purposes.

4.3 | Assessment of statistical parameters for detailed coefficients

For the normal condition and different percentages of the ISSCRF condition of the BLDC motor, the detail coefficients D_K , D_S , D_R have been determined as shown in Figure 8. It has been observed from Figure 8a that except only the D_K values for the seventh and ninth levels that are decreasing with the increase in the percentage of ISSCRF, all values are in a very zig-zag nature. After monitoring Figure 8b, it can be concluded that all the values of D_S are of a very zig-zag nature and no effective conclusion can be made from these values for fault diagnosis.

As shown in Figure 8c, it can be observed that only the values of D_R at decomposition levels 6 and 7 are increasing with the variation in the percentage of ISSCRF and the rest all the values are too much zig-zag in nature, which is not helpful for the fault assessment. So, only the D_K at the seventh and ninth levels of decomposition and the D_R at decomposition levels 6 and 7 can be useful for the fault assessment.

4.4 | Best parameter selection

From Figures 7 and 8, the probable best curves for fault diagnosis of ISSCRF in a BLDC motor have been selected

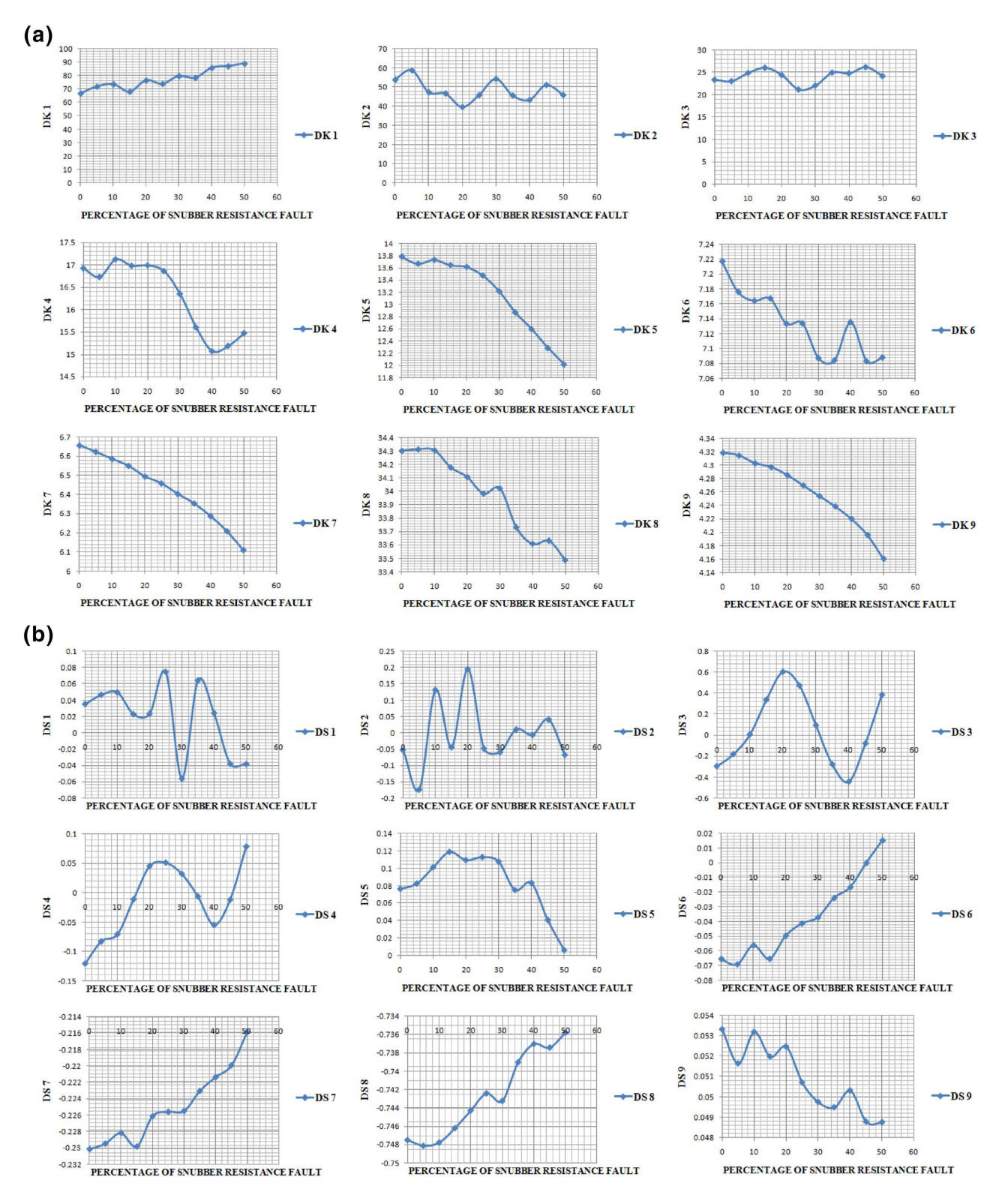


FIGURE 8 Kurtosis, skewness, RMS values of detailed coefficients versus the percentage of inverter switch snubber circuit resistance fault (ISSCRF).

(a) Kurtosis values of detailed coefficients versus the percentage of ISSCRF.

(b) Skewness values of detailed coefficients versus the percentage of ISSCRF.

(c) RMS values of detailed coefficients versus the percentage of ISSCRF.

as shown in Figure 9. After assessing, it can be concluded that the natures of curves of A_K , A_S at decomposition level 9 (expressed as A_{K9} and A_{S9} , respectively) are increasing,

whereas the curve of A_R at decomposition level 9 (expressed as A_{R9}) is decreasing with the increase in the percentage of ISSCRF. Also, it has been observed that the curve of D_K at

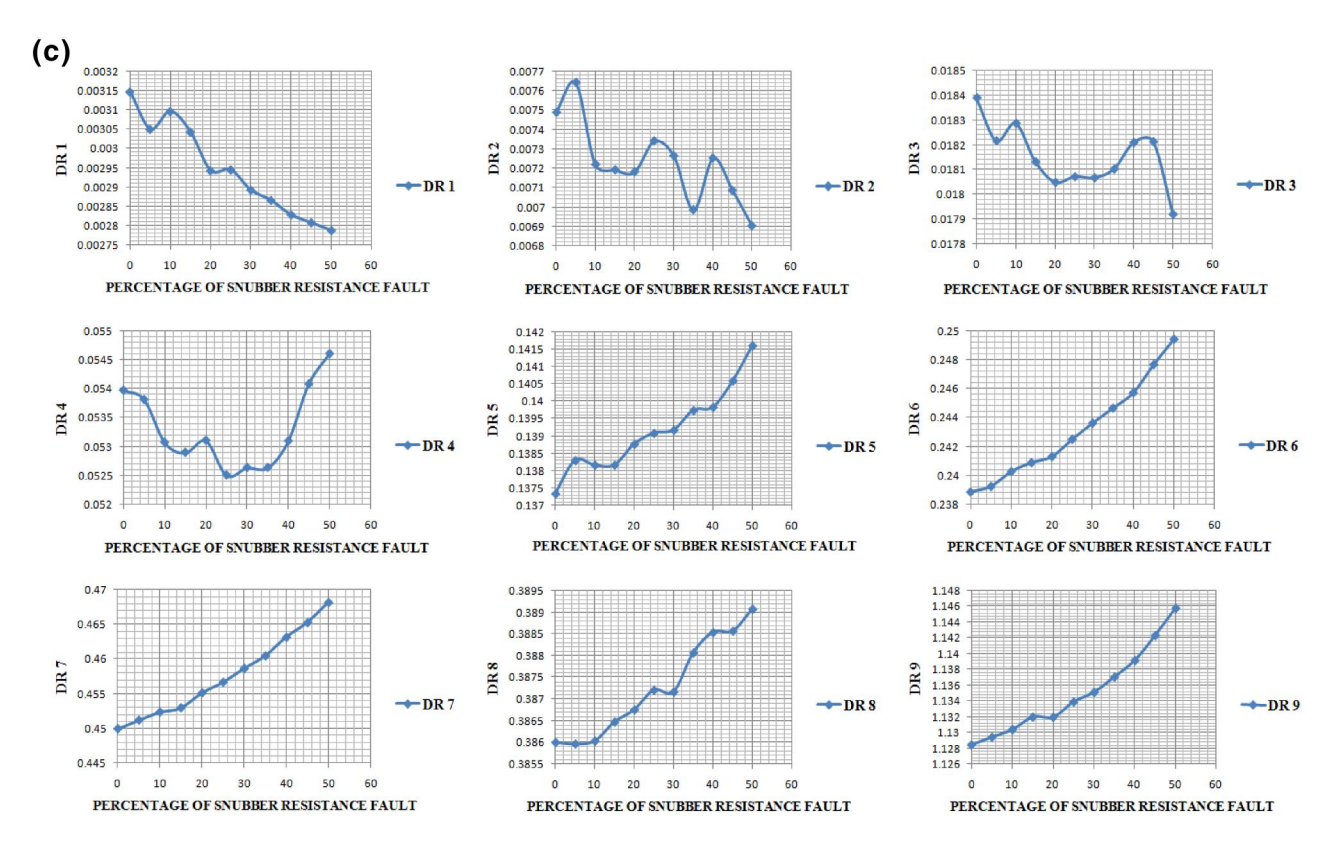


FIGURE 8 (Continued)

decomposition levels 7 and 9 (expressed as D_{K7} and D_{K9} , respectively) are decreasing and the natures of curves of D_R at decomposition levels 6 and 7 (expressed as D_{R6} and D_{R7} respectively) are increasing as the percentage of ISSCRF increases in a BLDC motor. Also, the natures of these curves are less zig-zag in nature as compared to the other curves.

5 | ALGORITHM, CASE STUDIES, AND VALIDATION

An algorithm for the detection of ISSCRF has been proposed as follows:

- (a) Capture the stator current signal.
- (b) Perform the DWT technique on the captured signal up to the decomposition level 9.
- (c) Now determine A_{K9} , A_{S9} , A_{R9} and D_{K7} , D_{K9} , D_{R6} and D_{R7} , respectively.
- (d) Detect the ISSCRF.

Here, experiments have been done on real three BLDC motors of known ratings and suffering from a known percentage value of ISSCRF for validation. The data obtained from these three real BLDC motors have been further used for the comparative study. The technical specifications along with the known percentage value of ISSCRF of the three BLDC motors used in three cases are given in Table 1.

The result of the comparative study done has been shown in Table 2. To find out the best technique for the detection of ISSCRF in the BLDC motor, errors have been calculated as shown in Table 2.

At last, a percentage error comparison has been done between these data and the result of the same has been shown in Figure 10.

For proper detection of ISSCRF, a modified algorithm has been proposed in this section as follows:

- (a) Capture the stator current signal of the BLDC motor.
- (b) Perform the DWT technique on the captured signal.
- (c) Determine D_{K7} .
- (d) Detect the ISSCRF.

This proposed process of detecting the percentage of ISSCRF has been shown in Figure 11. For fault detection of the ISSCRF, at first, the stator current of the BLDC motor has been captured. Then, DWT has been performed on the captured signal to determine the Kurtosis of detailed coefficient at decomposition level 7. Based on these Kurtosis values, ISSCRF, if exists, will be detected.

6 | COMPARISON AND NOVEL CONTRIBUTION

FFT-based diagnosis was done on the stator current of a BLDC motor and analyses on DC component, THD (%), the

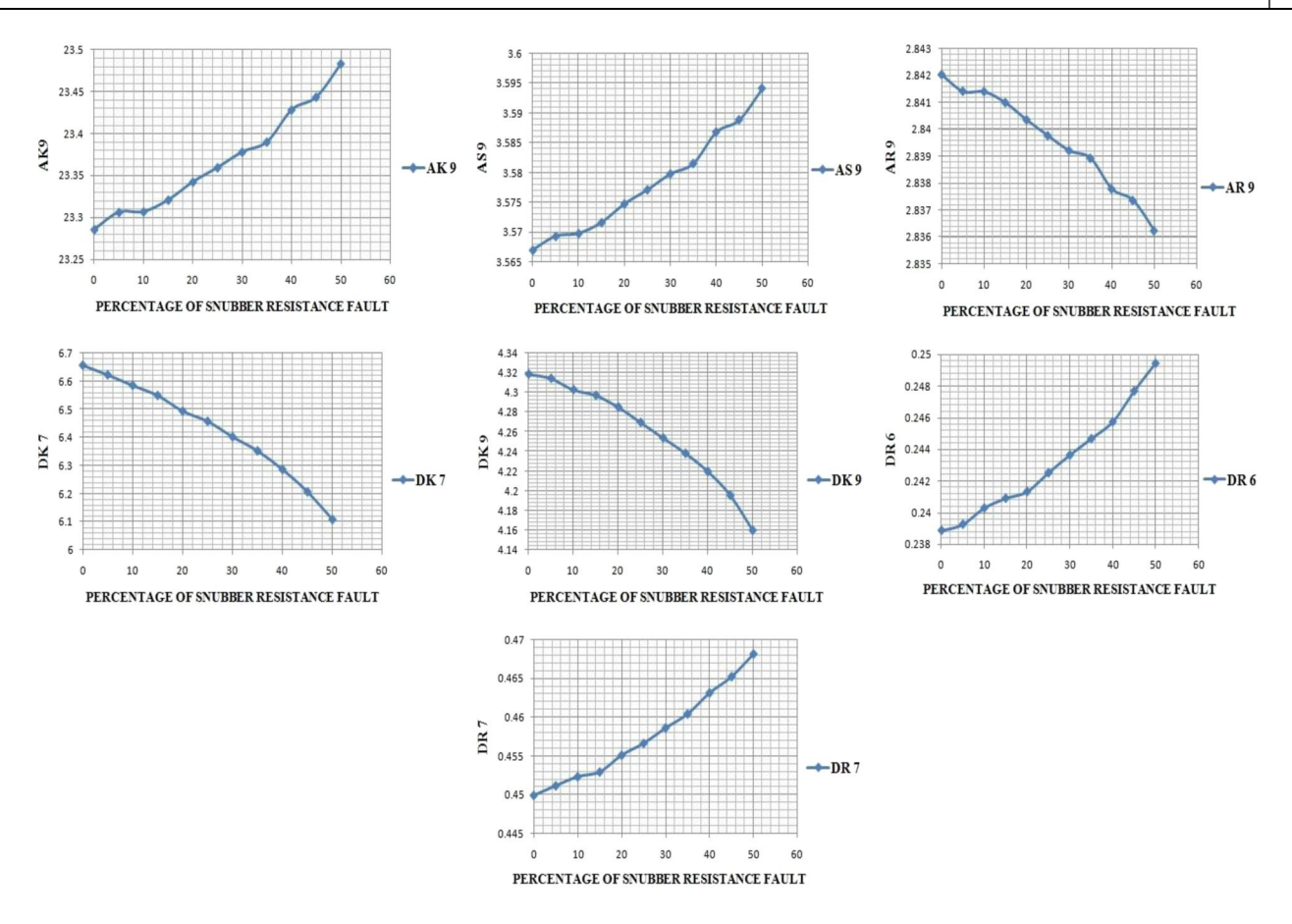


FIGURE 9 Selected curves for the assessment of percentage inverter switch snubber circuit resistance fault

TABLE 1 Technical specifications along with the known percentage value of inverter switch snubber circuit resistance fault of the three real brushless direct current motors

Parameter	Case-1	Case-2	Case-3
Resistance	0.36 Ω	0.45 Ω	0.20 Ω
Inductance	1.05 mH	1.4 mH	0.48 mH
Rotor inertia	$800~\mathrm{g~cm}^2$	$173~\mathrm{g~cm}^2$	$1600~\mathrm{g}~\mathrm{cm}^2$
Peak torque	2.1 N m	1.00 N m	4.2 N m
Rated power	220 W	133 W	440 W
Number of poles	8	4	8
Percentage of ISSCRF (%fault)	29%	37%	46%

Abbreviation: ISSCRF, inverter switch snubber circuit resistance fault

fundamental component of stator current of the BLDC motor have been observed in this paper during the normal condition and the different percentage values of ISSCRF. But it has been observed that from the FFT-based fault diagnosis, no specific outcome can be drawn for different percentages of ISSCRF.

Further, from DWT-based statistical parameters, it was observed that only $D_{\rm K}$ at the seventh and ninth levels and D_R at the sixth and seventh levels provide acceptable results that can be used for the detection of ISSCRF of the BLDC motor. But lastly, it has been clearly observed from the comparative

study done in Table 2 as well as from the percentage error comparison done in Figure 10 that only by using D_K at the seventh level, the value of the percentage of ISSCRF obtained gives the most satisfactory result.

So, after the overall comparison done between the results obtained from the FFT-based analyses and DWT-based analyses, it has been found that, firstly, the FFT-based analyses done on DC component, THD (%), the fundamental component of stator current of the BLDC motor do not give any specific outcome for the ISSCRF detection, and secondly, from the DWT-based fault diagnosis, the numerical values obtained by the simulation as well as real case studies have shown that the parameters, particularly kurtosis values of detailed coefficients at DWT decomposition level 7 (D_{K7}) have been found very effective for the ISSCRF detection. Therefore, in a BLDC motor, it is possible to detect ISSCRF using this detection technique.

Fault diagnosis found in the literature survey mainly deals with converter and motor faults. A comparison of this work and other related work has been carried out as presented in Table 3.

Thus, the specific novel outcome of this work is that it helps in inverter switch snubber circuit resistance fault detection very effectively using the statistical nature of wavelet-based detailed coefficients in terms of a kurtosis property instead of looking after DC component, fundamental component, total harmonic distortion and individual harmonic frequencies.

TABLE 2 Comparative study between experimental data obtained from real motors

Parameter	First case	Second case	Third case
%Fault (known)	29%	37%	46%
%Fault by using A_{K9}	$A_{K9} = 23.377$	$A_{K9} = 23.385$	$A_{K9} = 23.465$
	% Fault = 30%	% Fault = 34%	% Fault = 48%
	Error = -3.45%	Error = 8.11%	Error = -4.35%
%Fault by using A_{S9}	$A_{S9} = 3.578$	$A_{S9} = 3.584$	$A_{S9} = 3.591$
	% Fault = 27%	% Fault = 38%	% Fault = 47%
	Error = 6.90%	Error = -2.70%	Error = -2.17%
%Fault by using A_{R9}	$A_{R9} = 2.8396$	$A_{R9} = 2.8389$	$A_{R9} = 2.8374$
	% Fault = 26%	% Fault = 35%	% Fault = 45%
	Error = 10.34%	Error = 5.41%	Error = 2.17%
%Fault by using D_{K7}	$D_{K7} = 6.43$	$D_{K7} = 6.34$	$D_{K7} = 6.21$
	% Fault = 28%	% Fault = 36%	% Fault = 45%
	Error = 3.45%	Error = 2.70%	Error = 2.17%
%Fault by using D_{K9}	$D_{K9} = 4.26$	$D_{K9} = 4.24$	$D_{K9} = 4.20$
	% Fault = 28%	% Fault = 35%	% Fault = 45%
	Error = 3.45%	Error = 5.41%	Error = 2.17%
%Fault by using D_{R6}	$D_{R6} = 0.244$	$D_{R6} = 0.245$	$D_{R6} = 0.249$
	% Fault = 30%	% Fault = 36%	% Fault = 48%
	Error = -3.45%	Error = 2.70%	Error = -4.35%
%Fault by using D_{R7}	$D_{R7} = 0.459$	$D_{R7} = 0.462$	$D_{R7} = 0.465$
	% Fault = 31%	% Fault = 38%	% Fault = 44%
	Error = -6.90%	Error = -2.70%	Error = 4.35%

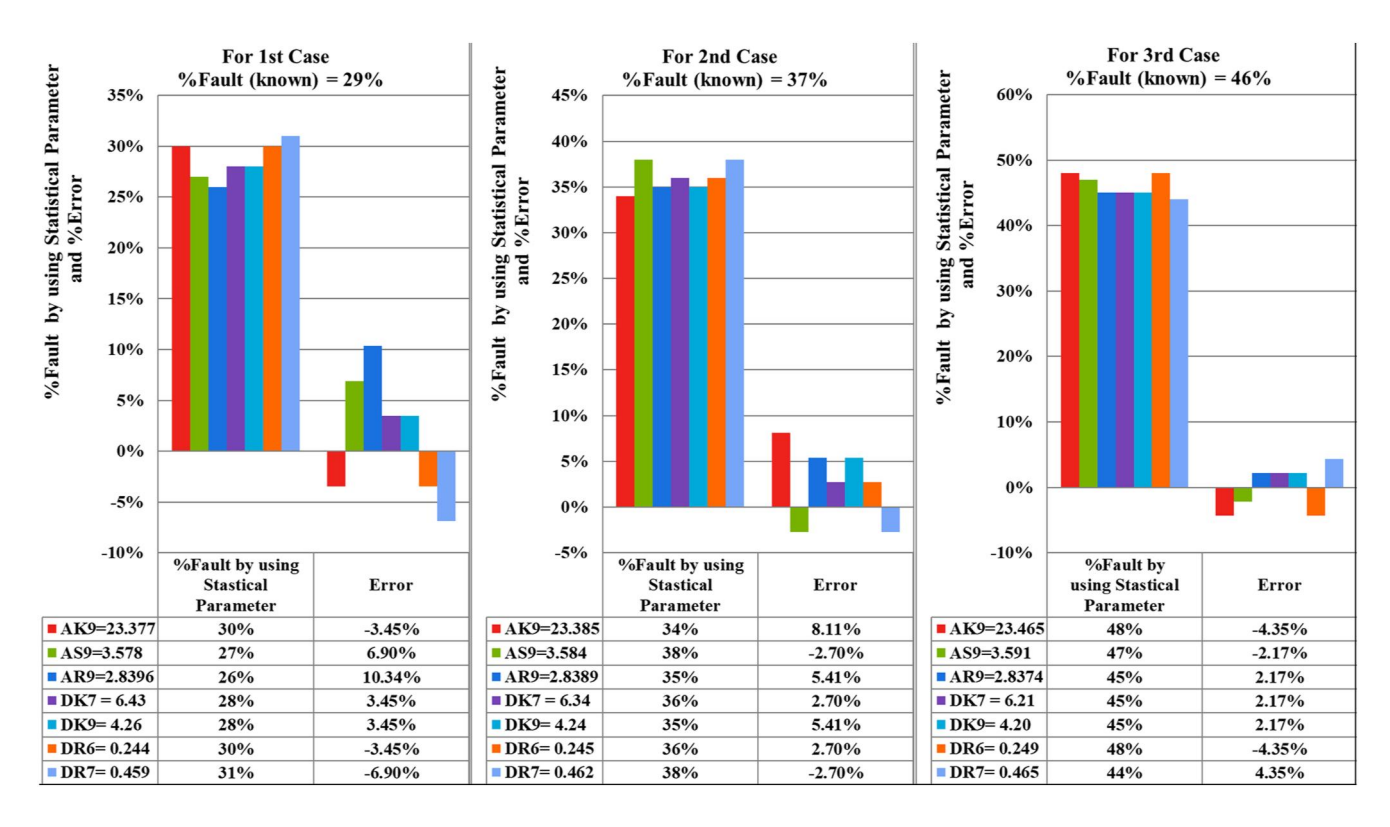


FIGURE 10 Percentage error comparison

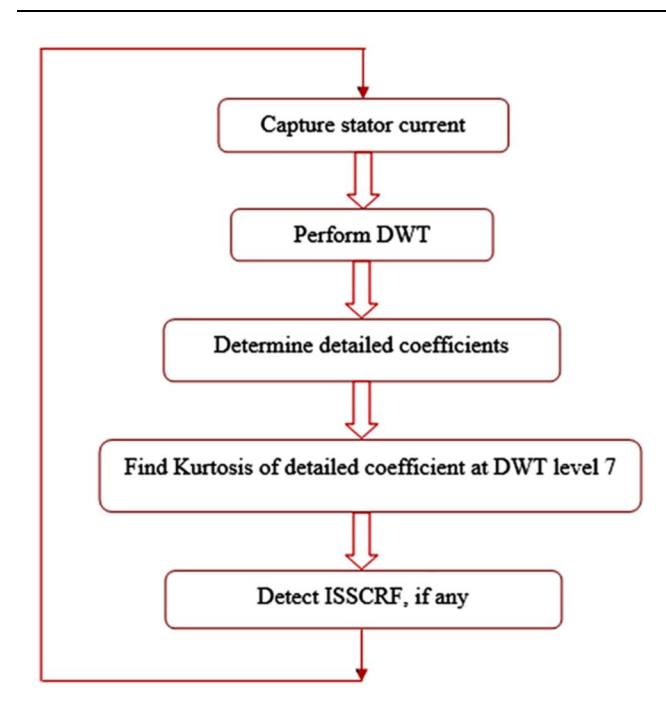


FIGURE 11 Process of obtaining the percentage of inverter switch snubber circuit resistance fault

TABLE 3 Comparative study

Reference	Method/parameters used	Outcomes
[9]	An MRAS-based diagnosis of fault in PWM voltage- source inverters	Open-circuit fault in PWM voltage-source inverters that may include snubber
[26]	Neural network and frequency components	Faults in voltage source inverter
[27]	The current magnitude and distortion	Investigation of snubber and protection circuits connections for power-electronic switch in hybrid DC circuit breaker
This work	FFT-based fundamental component FFT-based DC component FFT based THD	 Fault short diagnosis in snubber circuit used in BLDC motor drives Limitations are pointed out
	DWT-based detailed RMS DWT-based detailed skewness DWT-based detailed kurtosis	Best parameter extraction Diagnosis of short circuit fault of snubber circuit used in BLDC motor drives with high accuracy

Abbreviations: BLDC, brushless direct current; DWT, discrete wavelet transform.

7 | CONCLUSION

In this work, an FFT- and DWT-based statistical analysis has been carried out for ISSCRF diagnosis in snubber circuits connected with the BLDC motor. It was further observed that there are differences between the values of the parameters during normal and faulty conditions. The values of the parameters change with the increase in the percentage of ISSCRF. A comparison has been done between the data obtained both from FFT-based fault diagnosis and DWT-based fault diagnosis and also these are validated to find out the most accurate technique for the detection of ISSCRF in a BLDC motor. It has been observed that only the results of the kurtosis of detail coefficients at DWT decomposition level 7 (D_{K7}) have close similarities between them. Therefore, it is possible to detect an ISSCRF of a BLDC motor of any rating if the stator current is continuously monitored by the measurements and comparisons of values. Therefore, the diagnosis technique proposed here can be used very effectively to protect the system from expensive damages.

CONFLICT OF INTEREST

There is no conflict of interest with this paper.

ORCID

Sankha Subhra Ghosh https://orcid.org/0000-0002-6463-8156

Surajit Chattopadhyay https://orcid.org/0000-0001-5775-061X

REFERENCES

- Shabanian, A., et al.: Optimization of brushless direct current motor design using an intelligent technique. ISA (Instrum. Soc. Am.) Trans. 57, 311–321 (2015). https://doi.org/10.1016/j.isatra.2015.03.005
- Shirvani Boroujeni, M., Arab Markadeh, G.R., Soltani, J.: Torque ripple reduction of brushless DC motor based on adaptive input-output feedback linearization. ISA (Instrum. Soc. Am.) Trans. 70, 502–511 (2017). https://doi.org/10.1016/j.isatra.2017.05.006
- Gandolfo, D.C., et al.: Energy evaluation of low-level control in UAVs powered by lithium polymer battery. ISA (Instrum. Soc. Am.) Trans. 71(Part 2), 563–572 (2017). https://doi.org/10.1016/j.isatra.2017.08.010
- Li, H., Ning, X., Li, W.: Implementation of a MFAC based position sensorless drive for high-speed BLDC motors with nonideal back EMF. ISA (Instrum. Soc. Am.) Trans. 67, 348–355 (2017). https://doi.org/10. 1016/j.isatra.2016.11.014
- Batzel, T.D., Lee, K.Y.: Electric propulsion with the sensorless permanent magnet synchronous motor: model and approach. IEEE Trans. Energy Convers. 20(4), 818–825 (2005). https://doi.org/10.1109/TEC. 2005.847948
- Tashakori, A., Ektesabi, M.: Fault diagnosis of in-wheel BLDC motor drive for electric vehicle application. In: IEEE Intelligent Vehicles Symposium (IV), Gold Coast, Australia, 23–26 June 2013
- Liu, X.-Q., et al.: Fault detection and diagnosis of permanent-magnet DC motor based on parameter estimation and neural network. IEEE Trans. Ind. Electron. 47(5), 1021–1030 (2000)
- Li, J., et al.: Research on control strategies for ankle rehabilitation using parallel mechanism. Cogn. Comput. Syst. 2, 105–111 (2020). https://doi. org/10.1049/ccs.2020.0012
- Jung, S., et al.: An MRAS-based diagnosis of open-circuit fault in PWM voltage-source inverters for PM synchronous motor drive systems. IEEE Trans. Power Electron. 28(5), 2514–2526 (2013)
- Salehifar, M., et al.: Simplified fault-tolerant finite control set model predictive control of a five-phase inverter supplying BLDC motor in electric vehicle drive. Electr. Power Syst. Res. 132, 56–66 (2016). https:// doi.org/10.1016/j.epsr.2015.10.030
- Salehifar, M., Moreno-Eguilaz, M.: Fault faultinverter BLDC motor diagnosis and -tolerant finite control set-model predictive control of a multiphase voltage-source supplying. ISA (Instrum. Soc. Am.) Trans. 60, 143–155 (2016). https://doi.org/10.1016/j.isatra.2015.10.007

 Park, B.-G., et al.: Simple fault diagnosis based on operating characteristic of brushless direct-current motor drives. IEEE Trans. Ind. Electron. 58(5), 1586–1593 (2011)

- Fang, J., et al.: Online inverter fault diagnosis of buck-converter BLDC motor combinations. IEEE Trans. Power Electron. 30(5), 2674–2688 (2015). https://doi.org/10.1109/TPEL.2014.2330420
- Awadallah, M.A., Morcos, M.M.: Automatic diagnosis and location of open-switch fault in brushless DC motor drives using wavelets and neuro-fuzzy systems. IEEE Trans. Energy Convers. 21(1), 104–111 (2006)
- Moseler, O., Isermann, R.: Application of model-based fault detection to a brushless DC motor. IEEE Trans. Ind. Electron. 47(5), 1015–1020 (2000)
- Wang, Z., et al.: Application of augmented observer for fault diagnosis in rotor systems. Eng. Lett. 21(1), 10–17 (2013)
- Mondal, S., Chakraborty, G., Bhattacharyya, K.: Unknown input high gain observer for fault detection and isolation of uncertain systems. Eng. Lett. 17(2), 121–127 (2009)
- Misiti, M., et al.: Wavelet Toolbox for Use with MATLAB. The Mathworks, Inc., Natick (2000)
- Todd, P.C.: Snubber Circuits: Theory, Design and Application. Unitrode Corp. (1993). Technical Report. SLUP100 [Online] http://www.ti.com
- Prakash, S., Dhanasekaran, R.: Comparison of converter fed PMBLDC drive systems with and without Snubber. Int. J. Eng. Res. Appl. (IJERA). 3(4), 722–727 (2013)
- Rashid, M.H.: Power Electronics Circuits, Devices and Applications Seventh Impression. Pearson Education, New Delhi (2009)
- Karmakar, S., et al.: Induction Motor Fault Diagnosis, first edition. Springer, Singapore (2016)
- Antonino, J.A., et al.: Study of the start-up transient for the diagnosis of broken bars in induction motors: a review. http://www.aedie.org/ 9CHLIE-paper-send/318_Antonino.pdf
- Ray, D.K., Roy, T., Chattopadhyay, S.: Single and diagonal double thrust failure assessment of quad-copter at starting. Measurement 156, 1–13 (2020). https://doi.org/10.1016/j.measurement.2020.107591
- Chattopadhyay, A., Chattopadhyay, S., Sengupta, S.: Measurement of harmonic distortion and Skewness of stator current of induction motor at crawling in Clarke plane. IET Sc. Meas. Tech. 8(6), 528–536 (2014)

- Dhumale, R.B., Lokhande, S.D.: Neural network fault diagnosis of voltage source inverter under variable load conditions at different frequencies. Measurement. 91, 565–575 (2016). https://doi.org/10.1016/j. measurement.2016.04.051
- Yi, Q., et al.: An investigation of snubber and protection circuits connections for power-electronic switch in hybrid DC circuit breaker. In: 2019 IEEE 10th International Symposium on Power Electronics for Distributed Generation Systems (PEDG), Xi'an, pp. 43–46. (2019), https://doi.org/10.1109/PEDG.2019.8807706
- Iyer, A., et al.: Experimental validation of active snubber circuit for direct AC/AC converters. In: IEEE Energy Conversion Congress and Exposition (ECCE), Raleigh, NC, pp. 3856–3861. (2012). https://doi.org/10. 1109/ECCE.2012.6342283
- Zarghani, M., Mohsenzade, S., Kaboli, S.: A series stacked IGBT switch based on a concentrated clamp mode Snubber for pulsed power applications. IEEE Trans. Power Electron. 34(10), 9573–9584 (2019). https:// doi.org/10.1109/TPEL.2019.2894994
- Dong, S., et al.: Analysis and design of snubber circuit for Z-source inverter. In: 2014 16th European Conference on Power Electronics and Applications, Lappeenranta, pp. 1–10. (2014). https://doi.org/10. 1109/EPE.2014.6910870
- Matsushita, A., et al.: Inverter circuit with the regenerative passive snubber. In: Power Conversion Conference—Nagoya, Nagoya, pp. 167– 171. (2007). https://doi.org/10.1109/PCCON.2007.372963
- Kim, I.-D., et al.: A generalized Undeland snubber for flying capacitor multilevel inverter and converter. IEEE Trans. Ind. Electron. 51(6), 1290–1296 (2004). https://doi.org/10.1109/TIE.2004.837917

How to cite this article: Ghosh, S.S., Chattopadhyay, S., Das, A.: Fast Fourier transform and wavelet-based statistical computation during fault in snubber circuit connected with robotic brushless direct current motor. Cogn. Comput. Syst. 4(1), 31–44 (2022). https://doi.org/10.1049/ccs2.12041